ARTICLE

pubs.acs.org/Biomac

Antifouling Performance of Cross-linked Hydrogels: Refinement of an Attachment Model

Chelsea M. Magin,[†] John A. Finlay,[‡] Gemma Clay,[‡] Maureen E. Callow,[‡] James A. Callow,[‡] and Anthony B. Brennan*[,†,§]

[†]J. Crayton Pruitt Family Department of Biomedical Engineering, [‡]School of Biosciences, The University of Birmingham, Birmingham B15 2TT, U.K.

[§]Department of Materials Science & Engineering, University of Florida, Gainesville, Florida 32611, United States

Supporting Information

ABSTRACT: Poly(ethylene glycol) dimethacrylate (PEGDMA), PEGDMA-*co*-glycidyl methacrylate (PEGDMA-*co*-GMA), and PEGDMA-*co*-hydroxyethyl methacrylate (PEGDMA-*co*-HEMA) hydrogels were polymerized using ammonium persulfate and ascorbic acid as radical initiators. Surface energies of the hydrogels and a standard, poly(dimethylsiloxane) elastomer (PDMSe), were characterized using captive bubble and sessile drop measurements, respectively (γ = 52 mN/m, γ_0 = 19 mN/m). The chemical composition of the hydrogels was characterized by attenuated total reflectance Fourier transform infrared (ATR-FTIR) spectroscopy. All three hydrogel compositions reduced significantly (p = 0.05) initial attachment of zoospores of the green alga *Ulva linza* (up to 97%), cells of the diatom *Navicula incerta* (up to 58%) and the bacterium *Cobetia marina* (up to 62%), compared to a smooth PDMSe standard. A shear stress (45 Pa), generated in a water channel, eliminated up to 95% of the initially attached cells of *Navicula* from the smooth hydrogel surfaces relative to smooth PDMSe surfaces. Compared to the PDMSe standard, 79% of the cells of *C. marina* were removed from all smooth hydrogel compositions when exposed to a 50 Pa wall shear stress. Attachment of spores of the green alga *Ulva* to microtopographies replicated in PEGDMA-*co*-HEMA was also evaluated. The Sharklet AF microtopography patterned, PEGDMA-*co*-HEMA surfaces reduced attachment of spores of *Ulva* by 97% compared to a smooth PDMSe standard. The attachment densities of spores to engineered microtopographies in PDMSe and PEGDMA-*co*-HEMA were shown to correlate with a modified attachment model through the inclusion of a surface energy term. Attachment densities of spores of *Ulva* to engineered topographies replicated in a material other than PDMSe are now correlated with the attachment model (R^2 = 0.80).

INTRODUCTION

Biofouling (the accumulation of microorganisms, plants, and animals on a wetted surface) is a widespread problem in the maritime industry. The biofouling process typically begins with conditioning of the surface[1] and the development of microbial slime layers containing bacteria, diatoms (unicellular algae), and their extracellular products.[2−4] As these slime layers foul a vessel, hydrodynamic drag and consequently fuel consumption increase significantly.[5] Drag and fuel consumption increase further when macrofoulers, including macro-algae and invertebrates, colonize the surface.[5] The annual cost due to hull fouling fleet-wide for the United States Navy alone was estimated to be $180−$260 M on the basis of an analysis of the economic impact of biofouling on a class of naval surface ships.[6] Fouling of ship hulls is also a primary cause for the introduction and spread of nonindigenous marine species worldwide.[7−10] The green macro-alga (seaweed) *Ulva* is found all over the world and is well-known for fouling submerged structures such as ship hulls.[11] *Ulva* colonizes substrata by releasing large numbers of motile spores (zoospores) that must select a suitable surface and transition to attached, nonmotile spores before germinating to produce new plants. Surface selection is influenced by chemical, physicochemical,[12,13] biological,[14] and topographic[15,16] cues. Zoospores of *Ulva*, the cells of the diatom *Navicula incerta*, and the marine bacterium *Cobetia marina* are all used in this study as model soft fouling organisms representing three diverse phylogenetic groups, viz. the eukaryotic Plantae (*Ulva*), the eukaryotic Chromista (*Navicula*), and the prokaryotic Bacteria (*Cobetia*).[17]

Surface chemistry is an important factor in the adhesion and release of a fouling organism.[18,19] Self-assembled monolayers (SAMs) have been widely used to evaluate the influence of surface energy on attachment.[13,20−23] Experiments have shown that higher numbers of spores of *Ulva* attach to hydrophobic SAMs versus hydrophilic SAMs in static assays.[24] However, when attached spores were exposed to shear stress in a water channel, the attachment strength on hydrophilic SAMs was greater.[21] Materials composed of poly(ethylene glycol) (PEG) and its oligomers exhibit resistance to protein adsorption,[25,26] bacterial colonization,[27] and cell adhesion[28] and have been studied extensively for biomedical applications. These results have led mainly to the evaluation of non-cross-linked PEG SAMs, brushes, and grafts for marine antifouling applications.[29,30] The number of zoospores of *Ulva* and cells of *Navicula* firmly attached to SAMs of hexa(ethylene glycol)-containing alkanethiols with systematically changing end-group termination increased with decreasing wettability.[19] This increase in attachment has also

Received: October 14, 2010
Revised: February 21, 2011
Published: March 14, 2011

been correlated with an increase in adsorption of the protein fibrinogen.[30] Monolayers of high molar mass PEG (MW = 2 kg/mol, 5 kg/mol) SAMs resisted spore attachment.[8] Spores did not settle (attach) to the PEG monolayers, while on oligoethylene glycol SAMs, high numbers of spores settled and secreted adhesive but they could not bind to the surface so cells were easily washed off by slight disturbance. The difference in response to PEG versus OEG was ascribed to differences in hydration and steric repulsion.[8] Coatings consisting of PEG methacrylate (PEGMA) and 2-hydroxyethyl methacrylate (HEMA) grafted to glass slides were shown to exhibit antifouling and fouling release performance when tested against a wide range of organisms.[29]

Hydrogels, i.e., cross-linked polymer networks that swell in the presence of water, have also been studied for antifouling applications. Hydrogel surfaces of alginate, chitosan, and poly(vinyl alcohol) substituted with stilbazolium groups (PVA-SbQ) inhibited attachment of cypris larvae of *Balanus amphitrite*[31] and the marine bacterium *Pseudomonas* sp. NCIMB2021.[32] Hydrogels based on HEMA reduced fouling in two algal colonization bioassays and remained visually clean in field testing for up to 12 weeks with the addition of benzalkonium chloride, a biocidal compound.[33] Cross-linked poly(ethylene glycol) diacrylate hydrogels have also been evaluated as protein-resistant coatings. Surfaces that were more hydrophilic, on the basis of contact angle measurements, exhibited less protein adsorption.[34] A variety of cross-linked hydrogel compositions including poly(HEMA) were shown to reduce adhesion of cyprids of the barnacle *Balanus amphitrite*.[35]

Surface microtopographies created in poly(dimethylsiloxane) elastomer (PDMSe) have been proposed as a nontoxic strategy for inhibiting the settlement (initial attachment) of fouling organisms. A bioinspired surface topography, Sharklet AF, reduced attachment of zoospores of *Ulva* by 86% compared to smooth PDMSe.[36] An empirical relationship called the engineered roughness index (ERI) was developed to quantify topographical roughness on the basis of parameters that describe surface energy.[37] A negative correlation between the attachment of spores of *Ulva* and ERI was demonstrated[37] and a predictive attachment model[38] was developed on the basis of a revised version (ERI_{II}). Three topographies, including a new pattern called Recessed Sharklet AF were tested to show the predictive nature of the model.[38] Recessed Sharklet AF was intentionally designed with a higher ERI_{II} value and, as predicted, reduced the attachment of spores of *Ulva* compared to Sharklet AF.[38] Recently, an extension of the attachment model was reported that correlated the attachment densities of spores of *Ulva* and cells of *C. marina* with surface roughness by incorporating the Reynolds number of the organism into the model.[39]

To date, our studies of the influence of microtopography on the attachment of fouling organisms have been based mainly on patterned PDMSe. Since, as discussed above, nonpatterned brushes and hydrogels based on oligo- and poly ethylene glycols exhibit high degrees of resistance to the attachment of spores of *Ulva*, it is of interest to explore the effect of combining inhibitory microtopographies with alternative, cross-linked PEG-based hydrogels. Therefore, in the present study we have first evaluated the antifouling properties of a range of such chemistries. Cross-linked hydrogels in poly(ethylene glycol) dimethacrylate (PEGDMA), poly(ethylene glycol) dimethacrylate-*co*-glycidyl methacrylate (PEGDMA-*co*-GMA), and poly(ethylene glycol) dimethacrylate-*co*-hydroxyethyl methacrylate (PEGDMA-*co*-HEMA)

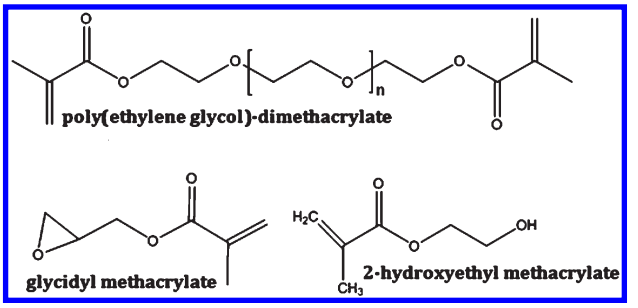

Figure 1. Chemical structures of monomers used to produce functionalized hydrogels.

were prepared by a thermal polymerization process using ammonium persulfate (APS) and ascorbic acid (AA) as radical initiators.[40,41] The PEGDMA-*co*-GMA hydrogel composition and a UV curing process were reported previously as a means to covalently graft proteins for studying cell adhesion.[40] The GMA chemistry facilitates adhesion of the hydrogels to epoxy coatings. Functionalizing the PEGDMA hydrogel with HEMA creates a material with the same average molar mass between cross-links as the PEGDMA-*co*-GMA and hence similar mechanical properties while retaining a surface chemistry similar to that of the PEGDMA composition. These chemistries create a self-supporting layer of cross-linked, hydrogel material that is much thicker than a graft or brush and can be microtopographically modified. Smooth hydrogels were evaluated for the influence of chemistry on antifouling performance. The composition that showed the highest inhibition of *Ulva* attachment was then microtopographically modified and evaluated to refine the attachment model. It was hypothesized that the attachment of spores of *Ulva* to engineered antifouling topographies created in hydrogel would have a negative linear correlation with the attachment model. A surface energy term was included in the model to expand applicability of this approach to materials beyond PDMSe.

EXPERIMENTAL SECTION

Materials. PEGDMA ($\overline{M_n}$ = 1 kg/mol), a difunctional polyethylene glycol macromonomer, was purchased from Polysciences Inc. (Warrington, PA). 2-Hydroxyethyl methacrylate 98% stabilized was purchased from Acros Organics (Geel, Belgium). Glycidyl methacrylate >97%, ascorbic acid (AA) 99+%, and ammonium persulfate were purchased from Sigma-Aldrich (Milwaukee, WI). (Methacryloxy) propyltriethoxysilane was purchased from Gelest Inc. (Morrisville, PA). Ultrapure water was produced by a Barnstead Nanopure Ultra Pure Water System (Waltham, MA). The base material for standards was a platinum-catalyzed PDMSe (Silastic T2; Dow Corning Corp.).

Sample Preparation. PEGDMA, PEGDMA-*co*-GMA, and PEGDMA-*co*-HEMA hydrogels were produced using a thermally activated polymerization. Aqueous solutions were prepared by combining 25 wt % PEGDMA ($\overline{M_n}$ = 1 kg/mol) used as is, 0.5 wt % ammonium persulfate and ascorbic acid as chemical initiators, and ultrapure water to balance. To create a functionalized PEGDMA hydrogel, 5 wt % of GMA or HEMA was added to the aqueous solution (Figure 1).

The hydrogels were produced as either free-standing films or coatings attached to 76 × 22 mm silanated microscope glass slides. Glass slides were pretreated with 0.5% (methacryloxy)propyltriethoxysilane in a 95% ethanol/water solution for 10 min, rinsed thoroughly with 95% ethanol, and dried at 120 °C for 15 min. Pretreated slides were soaked in toluene for 15 min to remove the polymerization inhibitor incorporated

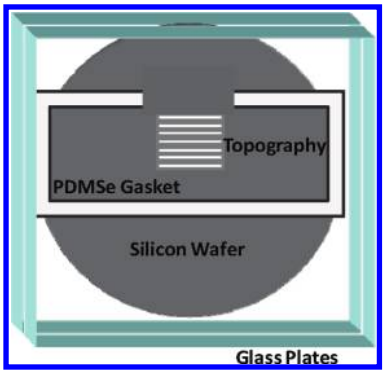

Figure 2. Schematic of mold for hydrogel production.

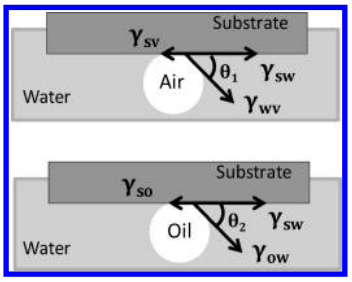

Figure 3. Schematic of captive air and oil bubble measurements for calculating surface energy.

into the silane coupling agent and air-dried. All prepolymer compounds were combined in a glass beaker and stirred until a solution was achieved; i.e., the PEGDMA was dissolved. The prepolymer solution was then poured into two centrifuge tubes and centrifuged for 10 min at 3300 rpm. The centrifuged prepolymer solution was pipetted into a mold (Figure 2). The mold contained a PDMSe gasket with an opening (2.5 cm × 7.6 cm × 2 mm) for a pretreated glass slide. The gasket was placed on top of a glass plate (12.7 cm × 12.7 cm × 0.32 cm), and the pretreated slide was fitted into the opening in the gasket. A microtopographically modified silicon wafer was placed on top of the PDMSe spacer, with the topography facing down, to create engineered microtopographies. Smooth samples were cast against a second glass plate. The mold was assembled by adding a second glass plate on the back of the silicon wafer and clamping with three 2 in. binder clips. The entire assembly was heated to 45 °C for 45 min.[41] Hydrogel-coated slides were removed from the assembly by peeling.

Two topographic molds, continuous channels 2.6 μm tall, 2 μm wide, and spaced by 2 μm (+2.6CH2 × 2) and the Sharklet AF pattern 2.8 μm tall, 2 μm wide, and spaced by 2 μm (+2.8SK2 × 2)[37] were replicated with this process.

To create smooth standards and topographically modified surfaces in PDMSe, the elastomer was prepared by mixing 10 parts by weight of resin and 1 part by weight curing agent. The mixture was stirred by hand for 5 min and degassed under vacuum (95 kPa) for 30 min to remove bubbles. An allyltrimethoxysilane-coupling agent was applied to clean glass microscope slides (0.5 wt % in 95% ethanol/water solution) and heated for 10 min at 120 °C. The Silastic T2 was then placed in contact with the treated slides in a mold consisting of two glass plates and aluminum spacers. The elastomer was polymerized at ambient temperature for 24 h. Topographically modified PDMSe samples were prepared in a two-step casting process previously described.[36]

Chemical Composition. Free standing films of PEGDMA, PEGDMA-*co*-GMA, and PEGDMA-*co*-HEMA were polymerized and air-dried for 48 h. The attenuated total reflectance Fourier transform infrared (ATR-FTIR) spectrum of each film was recorded on a Perkin-Elmer Spectrum One spectrometer. Spectra were obtained with a ZnSe crystal with an angle of incidence of 60° and resolution of 4 cm^{-1}. Twenty scans were performed for each sample. Spectral subtraction was performed to verify composition of the various hydrogel formulations.

Surface Energy Measurements. Captive air and oil bubble contact angles were measured to calculate the surface energy of the smooth, functionalized hydrogels (Figure 3). Two replicates of each hydrogel were cast onto glass slides. Both sides of five captive air bubbles and five captive *n*-octane bubbles were measured on each surface (n = 20). Surface energies were calculated using the method previously presented by Andrade.[42,43] Statistical differences between surfaces were evaluated using one-way analysis of variance (ANOVA) and Tukey's test for multiple comparisons (α = 0.05).

The surface energy of smooth PDMSe was measured using the Owens−Wendt−Kaelble approach.[44] The captive air bubble and captive oil bubble method of Andrade et al.[42] was not used to measure the surface energy of PDMSe because *n*-octane wetted the PDMSe surface, resulting in a contact angle that was not measurable. The method for obtaining surface energy should not change the value measured. Static contact angles of both sides of five drops of water, glycerol, and diiodomethane were measured on each of two replicates of smooth PDMSe (n = 20). The polar and dispersive components of the surface energy were calculated using two pairs of polar and nonpolar liquids: water and diiodomethane and glycerol and diiodomethane. The contact angles were reduced to surface energies by solving simultaneous equations and averaging the results.[44] The mean and standard deviation for the contact angles of each liquid were determined. However, since the measured values are related to each other by a system of simultaneous equations, it was not trivial to account for the covariance using a small sample size of matching pairs. Standard deviations were calculated using Minitab Statistical Software to randomly generate 1500 unit sample groups with the same mean and standard deviation as the measured sample groups. The systems of equations were solved multiple times with these data and the results were used for statistical analysis.

Microtopography Characterization. The +2.8SK2 × 2 and +2.6CH2 × 2 topographies (mold dimensions) were replicated as free-standing films in PEGDMA-*co*-HEMA and PDMSe. Hydrogel samples were immersed in deionized water for 24 h prior to characterization. Hydrogel samples in deionized water were prepared for scanning electron microscopy (SEM) by flash freezing with liquid nitrogen and subsequently freeze-drying for 5 d at 90 kPa and −42 °C (Lyph Lock 4.5 Freeze-Dry System, Labconco, Kansas City, MO). Freeze-dried hydrogel samples and PDMSe samples were mounted onto aluminum SEM stubs with double sided tape. These samples were sputter-coated with gold−palladium for 60 s at 38 mA. Samples were imaged with a JEOL JSM-6400 SEM with a tungsten filament at an accelerating voltage of 15 kV. Feature dimensions including height, width and spacing were measured using Image J software.

Biological Attachment Assays. Coated glass slides were shipped to the University of Birmingham overnight in 50 mL conical centrifuge tubes filled with deionized water. Samples were shipped in water to prevent the hydrogel layer from drying and cracking. Unlike other PEG-derivatized surfaces tested in Birmingham, these hydrogels are thick, self-supporting layers, not grafts or brushes. The hydrogels reach equilibrium swelling after 1 h and are not expected to exhibit extensive surface rearrangement due to the chemical cross-linking and relatively low average molar mass between cross-links. Prior to bioassay, the slides were transferred to sterile (0.22 μm filtered) artificial seawater (ASW) (Tropic Marin) for 2 h.

Ulva. A total of four *Ulva* attachment assays were performed. The first three assays were on smooth hydrogel slides. Six replicates of two topographies, +2.6CH2 × 2 and +2.8SK2 × 2 (mold dimensions), and smooth created in PEGDMA-*co*-HEMA and PDMSe were attached to

glass slides and provided for analysis in the fourth assay. Zoospores were obtained from fertile plants of *Ulva linza* collected from Llantwit Major (Wales) and prepared for attachment assays as described previously.[11] Briefly, each sample was immersed in 10 mL of a spore suspension containing 1.5×10^6 spores/mL and incubated in the dark for 45 min.

After unattached (motile) spores were washed away, attached spores on hydrogel and PDMSe slides were counted using a Zeiss Kontron 3000 imaging system attached to a Zeiss epi-fluorescence microscope with a 10x objective while the samples were still wet. Spores autofluoresce red due to chlorophyll.[45] Spore density was reported as the mean number of attached spores per mm^2 from 30 counts on each of the three replicates ±95% confidence intervals.

Navicula incerta. Cells of *Navicula incerta* were cultured in F/2 medium contained in 250 mL conical flasks until cells reached the logarithmic growth phase, approximately 3 days. Cells were washed three times in fresh medium before harvesting and diluting to give a suspension with a chlorophyll a content of approximately 0.25 μg/mL.[46] Six replicates of each hydrogel composition and PDMSe attached to glass slides were placed in Quadriperm dishes to which 10 mL of the diatom suspension was added. Cells were allowed to attach at ambient (~20 °C) on laboratory benches for 2 h. Samples were exposed to a submerged wash in seawater to remove cells that had not attached (the underwater immersion process avoided passing the samples through the air−water interface).

Three replicates were counted wet using the image analysis system described above. Counts were made for 30 fields of view (0.064 mm^2) on each sample. The remaining three replicate samples were exposed to a wall shear stress of 45 Pa in a water channel.[47] The number of cells remaining attached was counted.

C. marina. Cultures of *C. marina* (ATCC 25374)[48] were grown in marine broth contained in 100 mL conical flasks, at 18 °C on an orbital shaker at 60 rpm overnight. Cells were harvested by centrifugation (8000 rpm for 1 min) and washed two times in sterile (0.22 μm filtered) Tropic Marin ASW to remove any residual marine broth. The cells were resuspended in sterile ASW and briefly sonicated to aid dispersion. The suspension was diluted to an absorbance of 0.3 at 600 nm. Six replicates of each hydrogel composition and PDMSe attached to glass slides were placed in Quadriperm dishes to which 10 mL of the suspended bacteria were added. The dishes were incubated at ambient (~20 °C) on the laboratory bench for 2 h. After incubation, the slides were washed gently in seawater to remove unattached bacteria.

Three replicates were stained with crystal violet (0.01% in seawater) and counted under a 20× objective while still wet. Counts were made for 30 fields of view (2500 μm^2) on each sample. The remaining three replicates with attached bacteria were exposed to a wall shear stress of 50 Pa in a water channel.[47] The number of cells remaining attached was counted as described above. The cell density per mm^2 was calculated for each count ($n = 90$). The mean cell densities were compared using one-way analysis of variance (ANOVA) and Tukey's test for multiple comparisons.

RESULTS

Chemical Composition. Spectral subtraction of PEGDMA from PEGDMA-*co*-HEMA shows characteristic peaks for HEMA, i.e., 3400−3200 cm^{-1} (OH stretch), 2863−2843 cm^{-1} (CH symmetric stretch), 1750−1735 cm^{-1} (C═O stretch), 1485−1445 cm^{-1} (CH asymmetric deformation), and 1150−1060 cm^{-1} (C—O—C asymmetric stretch) (Figure S1, Supporting Information). Spectral subtraction of PEGDMA from PEGDMA-*co*-GMA shows characteristic bands for GMA at 1715−1740 cm^{-1} (C═O stretch), 1485−1445 cm^{-1} (CH deformation), 1280−1230 cm^{-1} (C—O—C symmetric stretch), and 950−815 cm^{-1} (asymmetric stretch) (Figure S2, Supporting Information).

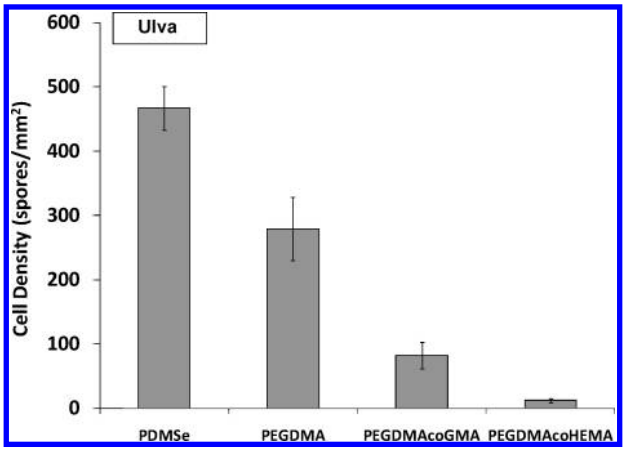

Figure 4. Smooth, functionalized poly(ethylene glycol)-based cross-linked hydrogels reduce the attachment density of zoospores of *Ulva*. These data are representative of three separate assays. Error bars indicate 95% confidence intervals.

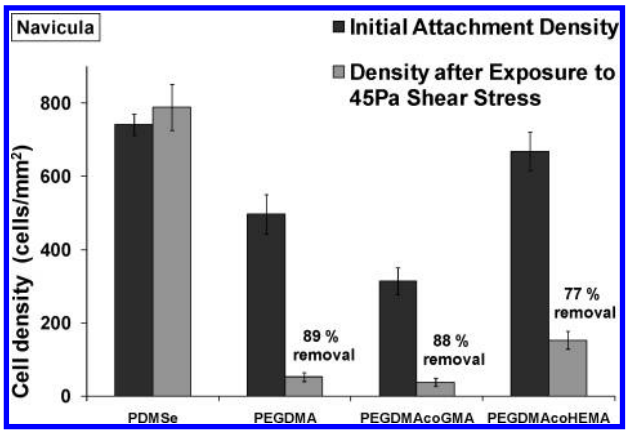

Figure 5. Smooth, functionalized poly(ethylene glycol)-based cross-linked hydrogels reduce density of attached cells and attachment strength of *Navicula*. Error bars indicate 95% confidence intervals.

Surface Energy Measurements. The surface energies of PEGDMA and PEGDMA-*co*-HEMA calculated from measured captive air and oil bubble contact angles were not statistically different ($\alpha = 0.05$, $p = 0.11$). The surface energy of PEGDMA-*co*-GMA was significantly higher than both PEGDMA and PEGDMA-*co*-HEMA ($\alpha = 0.05$, $p < 0$). The surface energies of all three hydrogels are higher than that of PDMSe (Tables S2 and S3, Supporting Information).

Biological Attachment Assays. Results representative of three separate assays showed that smooth PEGDMA, PEGDMA-*co*-GMA, and PEGDMA-*co*-HEMA reduced the attachment of spores of *Ulva* compared to smooth PDMSe (Figure 4). The average spore density on smooth PDMSe was calculated to be 467 ± 33 spores/mm^2. Lower mean densities were measured on PEGDMA (279 ± 49) and PEGDMA-*co*-GMA (82 ± 20), with the lowest mean density measured on PEGDMA-*co*-HEMA (12 ± 3). In separate hydrodynamic assays of adhesion strength, the average percent removal of attached spores from both smooth PDMSe and PEGDMA was approximately 40% (data not shown). There was no removal from smooth PEGDMA-*co*-GMA and

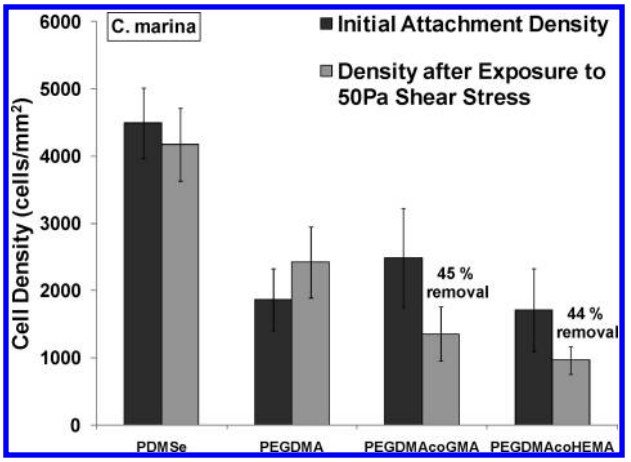

Figure 6. Smooth, functionalized poly(ethylene glycol)-based hydrogels reduce attachment density and attachment strength of *C. marina*. Error bars indicate 95% confidence intervals.

PEGDMA-*co*-HEMA although this result must be treated with caution because removal is expressed as a percentage of the low numbers of spores initially settled on these two hydrogels. However, it is possible to conclude in general terms that these two hydrogel chemistries do not have intrinsic fouling-release properties for spores of *Ulva*.

Diatom cells, unlike spores of *Ulva*, are not motile in the water column. The cells come into contact with a surface by gravity and water currents so at the end of a 2 h incubation period, approximately the same number of diatoms will be in contact with all test surfaces. Differences in the density of attached cells of *Navicula* were quantified following a gentle underwater washing, which removed cells that were in contact with, but not attached to, the surface. The initial attachment density was lowest on smooth PEGDMA-*co*-GMA, which was significantly lower than initial attachment densities on smooth PEGDMA, PDMSe, and PEGDMA-*co*-HEMA ($\alpha = 0.05$, $p < 0$) (Figure 5). Initial attachment densities on smooth PDMSe and PEGDMA-*co*-HEMA were not statistically different ($\alpha = 0.05$). Exposure to a shear stress of 45 Pa in a water channel caused 77% or more of diatom cells that were attached after gentle washing to be removed from all hydrogel surfaces (Figure 5). No cells were removed from the smooth PDMSe surface. The total percent reduction after removal for smooth PEGDMA-*co*-GMA compared to smooth PDMSe was 95%.

The initial attachment density of cells of *C. marina* was reduced on smooth hydrogels compared to a smooth PDMSe standard (up to 62%) with lowest densities on PEGDMA and PEGDMA-*co*-HEMA (Figure 6). Initial attachment densities of *C. marina* were not statistically different among the three smooth hydrogel compositions, but all hydrogels significantly reduced attachment versus PDMSe ($\alpha = 0.05$, $p < 0$). Exposure to a 50 Pa shear stress in a water channel caused 44% and 45% removal from PEGDMA-*co*-GMA and PEGDMA-*co*-HEMA, respectively (Figure 6). There was no statistically significant removal of *C. marina* from PDMSe or PEGDMA. The cell density on PEGDMA-*co*-HEMA after exposure to a 50 Pa shear stress was 77% less than that on PDMSe.

While smooth films of all three hydrogel chemistries significantly reduced the initial attachment of spores of *Ulva* compared to smooth PDMSe, PEGDMA-*co*-HEMA was the most effective and offered superior properties with respect to adhesion and functionalization as discussed above. It was therefore selected as the substrate for micropatterning and further testing. Channels and Sharklet AF topographies were replicated in PEGDMA-*co*-HEMA and PDMSe, characterized, and then evaluated in the standard attachment assay with spores of *Ulva*.

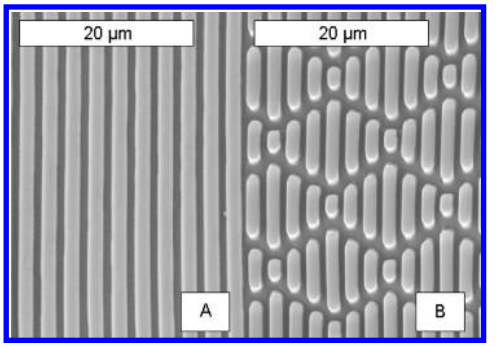

Figure 7. Scanning electron micrographs of (A) channels and (B) Sharklet AF topographies replicated in PEGDMA-*co*-HEMA hydrogel and freeze-dried.

Microtopography Characterization. The fidelity of topographic features replicated in PEGDMA-*co*-HEMA (Figure 7) and PDMSe was evaluated with SEM. All feature dimensions were measured using ImageJ (Table S1, Supporting Information).

***Ulva* Attachment.** The initial spore attachment density was reduced on both PDMSe channels and Sharklet AF topographies versus smooth PDMSe. Smooth PEGDMA-*co*-HEMA reduced spore attachment by an average of 75% compared to smooth PDMSe. Topographies produced in PEGDMA-*co*-HEMA reduced spore attachment by an average of 82% for channels and 93% for Sharklet AF compared to smooth PDMSe.

DISCUSSION

Hydrogel Characterization. Spectral subtraction of ATR-FTIR spectra verified the presence of GMA and HEMA in functionalized PEGDMA hydrogels. Contact angle measurements and surface energy calculations showed that the surface energy of PEGDMA-*co*-GMA was significantly higher than both PEGDMA and PEGDMA-*co*-HEMA (Tukey test $\alpha = 0.05$). The surface energies of PEGDMA and PEGDMA-*co*-HEMA were not significantly different statistically. SEM was used to confirm that topographies were replicated in hydrogel with high fidelity. Hydrogel compositions and polymerization conditions were specifically selected so that the water content of the hydrogels immediately after polymerization was approximately equal to the equilibrium water content to reduce feature size distortion due to swelling.

Biological Attachment Assays. Initial attachment density and attachment strength of marine fouling organisms have been attributed to many factors including surface chemistry[12,13,49−51] and surface topography.[16,36,38,39,45,52−55] The surface energy of all three PEGDMA-based hydrogels was more than twice that of the PDMSe standard in this report. Initial attachment densities of all three marine organisms were lower on the cross-linked hydrogels as compared to the PDMSe standard. These findings are consistent with results from other linear PEG-based materials that have been evaluated.[13,29,56] The low number of spores of *Ulva* removed from the hydrogel surfaces was also expected on the basis of the observation that spores generally attach more

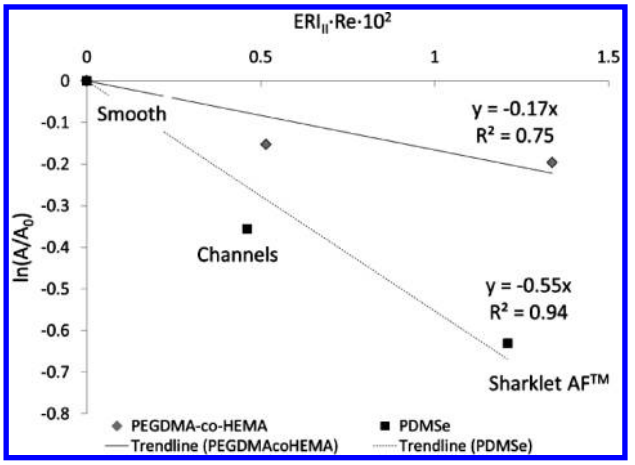

Figure 8. Normalized, transformed *Ulva* attachment density on PDMSe and PEGDMA-*co*-HEMA topographies plotted versus ERI$_{II}$·*Re*·10^2. Attachment density on PDMSe and PEGDMA-*co*-HEMA correlated with the equation that describes the attachment model (R^2 = 0.94 and R^2 = 0.75, respectively).

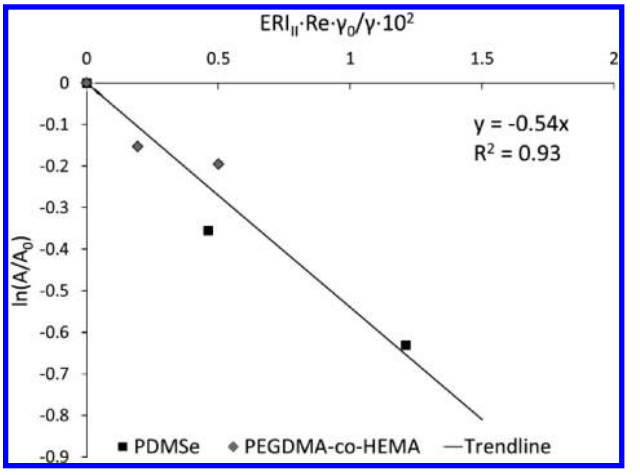

Figure 9. Normalized, transformed spore attachment density on PDMSe and PEGDMA-*co*-HEMA topographies plotted versus ERI$_{II}$·Re·γ/ γ_0*10^2. Attachment density on PDMSe and PEGDMA-*co*-HEMA show a negative, linear correlation with the attachment model multiplied by γ/ γ_0 (R^2 = 0.93).

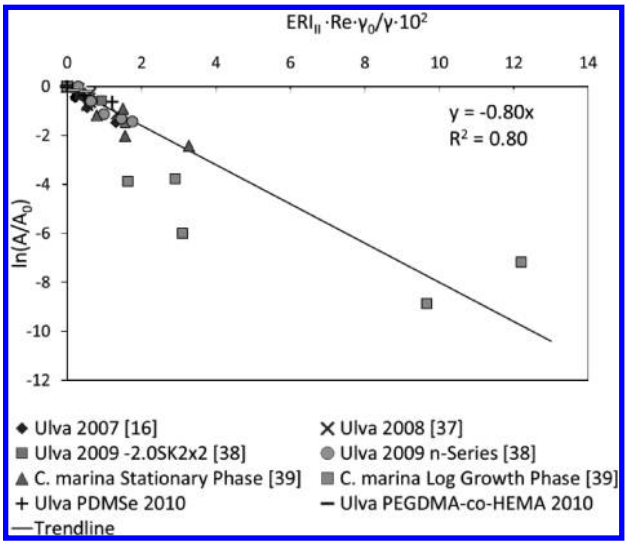

Figure 10. Normalized, transformed attachment densities of spores of *Ulva*[16,37,38] and cells of *C. marina*[39] on PDMSe and PEGDMA-*co*-HEMA topographies plotted versus ERI$_{II}$·*Re*·γ/γ_0·10^2. Attachment densities on PDMS e and PEGDMA-*co*-HEMA for eight different assays show a negative, linear correlation with ERI$_{II}$·*Re*·γ/γ_0·10^2 (R^2 = 0.80).

firmly to hydrophilic compared to hydrophobic surfaces.[57] All hydrogel compositions reduced the attachment strength of cells of the diatom *Navicula* compared to smooth PDMSe. Diatoms, unlike *Ulva*, have been found to adhere more firmly to hydrophobic surfaces including silicone elastomers,[46] self-assembled monolayers (SAMs),[58] and xerogels,[59] than to hydrophilic surfaces.

In the present paper, the smooth, functionalized compositions of PEGDMA-*co*-GMA and PEGDMA-*co*-HEMA reduced attachment strength of *C. marina* compared to PDMSe. These results are consistent with the "Baier curve", a plot that demonstrates the relationship between substratum surface tension and the degree of biological fouling retention.[60] There are two minima observed on the Baier curve, one between 20 and 30 mN/m and another between 50 and 70 mN/m. The surface tensions of PDMSe and the hydrogel substrates used in the present study were within these ranges and both exhibited low retention of fouling organisms. On the basis of these results, PEGDMA-*co*-GMA and PEGDMA-*co*-HEMA, in particular, are more effective fouling-release coatings than PDMSe for cells of *Navicula* and *C. marina*.

In a previous study the attachment densities of spores of *Ulva* and cells of *C. marina* to various topographies created in PDMSe were correlated with an attachment model.[39] The attachment model equation relates the attachment density on a particular topography (A) normalized by the attachment density on a smooth surface of the same chemistry (A_0) to the engineered roughness index (ERI$_{II}$) and the Reynolds number of the fouling organism (Re) (eqs 1 and 2).

$$\ln\left(\frac{A}{A_0}\right) = -m\cdot \mathrm{ERI}_{II} \qquad (1)$$

$$m = m'\cdot Re \qquad (2)$$

It has also been shown that attachment density on a variety of topographies in PDMSe can be predicted by this model.[38] Figure 8 demonstrates that this prediction can be extended to include topographies patterned in materials other than PDMSe since the attachment densities of spores of *Ulva* on PDMSe and PEGDMA-*co*-HEMA topographies correlated with eqs 3 and 4, respectively, when plotted in the form of the attachment model.

$$\ln\left(\frac{A}{A_0}\right) = -0.55\times 10^{-2}\cdot \mathrm{ERI}_{II} \qquad (3)$$

$$\ln\left(\frac{A}{A_0}\right) = -0.17\times 10^{-2}\cdot \mathrm{ERI}_{II} \qquad (4)$$

The discrepancy in the slopes of the attachment model may be attributed to the different surface energies of the materials. The effect was therefore incorporated into the attachment model by multiplying by the surface energy of the smooth substrate (γ) for each material normalized by the surface energy of PDMSe (γ_0).

The attachment densities on both PDMSe and PEGDMA-*co*-HEMA correlated (R^2 = 0.93) with the attachment model multiplied by the measured surface energy ratio (γ/γ_0) (Figure 9). The new slope of the attachment model (m) and the negative linear correlation are described by eqs 5 and 6.

$$m = m'' \cdot Re \cdot \frac{\gamma}{\gamma_0} \quad (5)$$

$$\ln\left(\frac{A}{A_0}\right) = \left(m'' \cdot Re \cdot \frac{\gamma}{\gamma_0}\right) \cdot \mathrm{ERI_{II}} \quad (6)$$

The results of eight assays with spores of *Ulva* and two assays with *C. marina* on various engineered microtopographies created in PDMSe and PEGDMA-*co*-HEMA correlated to the $\mathrm{ERI_{II}}$ with a new slope that consists of the *Re* of the organisms multiplied by a ratio of the surface energy measured on a smooth substrate to that of a standard (PDMSe) (R^2 = 0.80) (Figure 10).

CONCLUSION

The environmental and economic costs of biofouling have led to a need for environmentally neutral antifouling technologies.[19] The results from attachment studies performed with three fouling organisms on functionalized, cross-linked PEGDMA hydrogels provide insight that will lead potentially to improvements in antifouling and fouling release technologies. The slope of the attachment model as an indicator of an organism's sensitivity to a surface was extended by incorporating a ratio of the measured surface energy of a smooth substratum to that of a standard (PDMSe) into the attachment model. The attachment model has now been shown to correlate with the attachment density of spores of *Ulva* on two substrate materials, i.e., PDMSe and cross-linked PEGDMA hydrogels. Functionalized, smooth, cross-linked PEGDMA hydrogels reduced attachment of fouling organisms from three evolutionarily diverse groups (Plantae, Chromista, and Bacteria).

ASSOCIATED CONTENT

Supporting Information. Detailed results from microtopography characterization (Table S1) and ATR-FTIR spectra. Tables of surface energy measurements and contact angle measurements. This material is available free of charge via the Internet at http://pubs.acs.org.

ACKNOWLEDGMENT

C.M.M., J.A.F., G.C., M.E.C., J.A.C., and A.B.B. gratefully acknowledge the financial support of the Office of Naval Research (Contract no. N00014-10-1-0579 to C.M.M. and A. B.B. and Contract no. N00014-08-1-0010 to M.E.C. and J.A.C.). Special thanks to Sean Royston for his technical assistance in sample production and Kern Hast for performing PDMSe surface energy measurements and calculations. Thanks to Adwoa Baah-Dwomoh, Scott P. Cooper, and Julian Sheats for repeating hydrogel freeze-drying and SEM imaging.

REFERENCES

(1) Jain, A.; Bhosle, N. B. *Biofouling* **2009**, *25*, 13–19.
(2) Molino, P. J.; Childs, S.; Hubbard, M. R. E.; Carey, J. M.; Burgman, M. A.; Wetherbee, R. *Biofouling* **2009**, *25*, 149–162.
(3) Molino, P. J.; Campbell, E.; Wetherbee, R. *Biofouling* **2009**, *25*, 685–694.
(4) Molino, P. J.; Wetherbee, R. *Biofouling* **2008**, *24*, 365–379.
(5) Schultz, M. P. *Biofouling* **2007**, *23*, 331–341.
(6) Schultz, M.; Bendick, J.; Holm, E.; Hertel, W. *Biofouling* **2011**, *27*, 87–98.
(7) Otani, M.; Oumi, T.; Uwai, S.; Hanyuda, T.; Prabowo, R. E.; Yamaguchi, T.; Kawai, H. *Biofouling* **2007**, *23*, 277–286.
(8) Pettengill, J. B.; Wendt, D. E.; Schug, M. D.; Hadfield, M. G. *Biofouling* **2007**, *23*, 161–169.
(9) Piola, R. R.; Johnston, E. L. *Biofouling* **2008**, *24*, 145–155.
(10) Yamaguchi, T.; Prabowo, R. E.; Ohshiro, Y.; Shimono, T.; Jones, D.; Kawai, H.; Otani, M.; Oshino, A.; Inagawa, S.; Akaya, T.; Tamura, I. *Biofouling* **2009**, *25*, 325–333.
(11) Callow, M. E.; Callow, J. A.; Pickett-Heaps, J. D.; Wetherbee, R. *J. Phycol.* **1997**, *33*, 938–947.
(12) Ederth, T.; Pettitt, M. E.; Nygren, P.; Du, C.-X.; Ekblad, T.; Zhou, Y.; Falk, M.; Callow, M. E.; Callow, J. A.; Liedberg, B. *Langmuir* **2009**, *25*, 9375–9383.
(13) Schilp, S.; Rosenhahn, A.; Pettitt, M. E.; Bowen, J.; Callow, M. E.; Callow, J. A.; Grunze, M. *Langmuir* **2009**, *25*, 10077–10082.
(14) Joint, I.; Tait, K.; Callow, M. E.; Callow, J. A.; Milton, D.; Williams, P.; Camara, M. *Science* **2002**, *298*, 1207.
(15) Schumacher, J. F.; Aldred, N.; Callow, M. E.; Finaly, J. A.; Callow, J. A.; Clare, A. S.; Brennan, A. B. *Biofouling* **2007**, *23*, 307–317.
(16) Schumacher, J. F.; Long, C. J.; Callow, M. E.; Finaly, J. A.; Callow, J. A.; Brennan, A. B. *Langmuir* **2008**, *24*, 4931–4937.
(17) Cavalier-Smith, T. *Proc. R. Soc. London B* **2004**, *271*, 1251–1262.
(18) Rosenhahn, A.; Schilp, S.; Kreuzer, H. J.; Grunze, M. *Phys. Chem. Chem. Phys.* **2010**, *12*, 4275–4286.
(19) Magin, C. M.; Cooper, S. P.; Brennan, A. B. *Mater. Today* **2010**, *13*, 36–44.
(20) Bowen, J.; Pettitt, M. E.; Kendall, K.; Leggett, G. J.; Preece, J. A.; Callow, M. E.; Callow, J. A. *J. R. Soc. Interface* **2007**, 4.
(21) Finlay, J. A.; Callow, M. E.; Ista, L. K.; Lopez, G. P.; Callow, J. A. *Integr. Comp. Biol.* **2002**, *42*, 1116–1122.
(22) Ista, L. K.; Mendez, S.; Lopez, G. P. *Biofouling* **2010**, *26*, 111–118.
(23) Zhao, C.; Brinkhoff, T.; Burchardt, M.; Simon, M.; Wittstock, G. *Ocean Dynam.* **2009**, *59*, 305–315.
(24) Callow, M. E.; Callow, J. A.; Ista, L. K.; Coleman, S. E.; Nolasco, A. C.; Lopez, G. P. *Appl. Environ. Microbiol.* **2000**, *66*, 3249–3254.
(25) Ostuni, E.; Chapman, R. G.; Liang, M. N.; Meluleni, G.; Pier, G.; Ingber, D. E.; Whitesides, G. M. *Langmuir* **2001**, *17*, 6336–6343.
(26) Jeon, S. I.; Lee, J. H.; Andrade, J. D.; De Gennes, P. G. *J. Colloid Interface Sci.* **1991**, *142*, 149–158.
(27) Wagner, V. E.; Koberstein, J. T.; Bryers, J. D. *Biomaterials* **2004**, *25*, 2247–2263.
(28) Bozukova, D.; Pagnoulle, C.; De Pauw-Gillet, M.-C.; Ruth, N.; Jerome, R.; Jerome, C. *Langmuir* **2008**, *24*, 6649–6658.
(29) Ekblad, T.; Bergstrom, G.; Ederth, T.; Conlan, S. L.; Mutton, R.; Clare, A. S.; Wang, S.; Liu, Y.; Zhao, Q.; D'Souza, F.; Donnelly, G. T.; Willemsen, P. R.; Pettitt, M. E.; Callow, M. E.; Callow, J. A.; Liedberg, B. *Biomacromolecules* **2008**, *9*, 2775–2783.
(30) Schilp, S.; Kueller, A.; Rosenhahn, A.; Grunze, M.; Pettitt, M. E.; Callow, M. E.; Callow, J. A. *Biointerphases* **2007**, *2*, 143–150.
(31) Rasmussen, K.; Willemsen, P. R.; Ostgaard, K. *Biofouling* **2002**, *18*, 177–191.
(32) Rasmussen, K.; Ostgaard, K. *Water Res.* **2003**, *37*, 519–524.
(33) Cowling, M. J.; Hodgkiess, T.; Parr, A. C. S.; Smith, M. J.; Marrs, S. J. *Sci. Total Environ.* **2000**, *258*, 129–137.
(34) Ju, H.; McCloskey, B. D.; Sagle, A. C.; Kusuma, V. A.; Freeman, B. D. *J. Membr. Sci.* **2009**, *330*, 180–188.
(35) Murosaki, T.; Noguchi, T.; Kakugo, A.; Putra, A.; Kurokawa, T.; Furukawa, H.; Osada, Y.; Gong, J. P.; Nogata, Y.; Matsumura, K.; Yoshimura, E.; Fusetani, N. *Biofouling* **2009**, *25*, 313–320.

(36) Carman, M. L.; Estes, T. G.; Feinberg, A. W.; Schumacher, J. F.; Wilkerson, W.; Wilson, L. H.; Callow, M. E.; Callow, J. A.; Brennan, A. B. *Biofouling* **2006**, *22*, 11–21.
(37) Schumacher, J. F.; Carman, M. L.; Estes, T. G.; Feinberg, A. W.; Wilson, L. H.; Callow, M. E.; Callow, J. A.; Finlay, J. A.; Brennan, A. B. *Biofouling* **2007**, *23*, 55–62.
(38) Long, C. J.; Schumacher, J. F.; Robinson, P., II; Finaly, J. A.; Callow, M. E.; Callow, J. A.; Brennan, A. B. *Biofouling* **2010**, *26*, 411–419.
(39) Magin, C. M.; Long, C. J.; Cooper, S. P.; Ista, L. K.; Lopez, G. P.; Brennan, A. B. *Biofouling* **2010**, *26*, 719–727.
(40) Pfister, P. M.; Wendlandt, M.; Neuenschwander, P.; Suter, U. W. *Biomaterials* **2007**, *28*, 567–575.
(41) Shin, H.; Temenoff, J. S.; Mikos, A. G. *Biomacromolecules* **2003**, *4*, 552–560.
(42) Andrade, J.; King, R.; Gregonis, D.; Coleman, D. *J. Polym. Sci.: Polym. Symp.* **1979**, *66*, 313–336.
(43) Hu, D. S.-G.; Tsai, C.-e. *J. Appl. Polym. Sci.* **1996**, *59*, 1809–1817.
(44) Owens, D. K.; Wendt, R. C. *J. Appl. Polym. Sci.* **1969**, *13*, 1741–1747.
(45) Callow, M. E.; Jennings, A. R.; Brennan, A. B.; Seegert, C. A.; Gibson, A. L.; Wilson, L. H.; Feinberg, A. W.; Baney, R.; Callow, J. A. *Biofouling* **2002**, *18*, 237–245.
(46) Holland, R.; Dugdale, T.; Wetherbee, R.; Brennan, A.; Finlay, J. A.; Callow, J. A.; Callow, M. E. *Biofouling* **2004**, *20*, 323–329.
(47) Schultz, M. P.; Finlay, J. A.; Callow, M. E.; Callow, J. A. *Biofouling* **2000**, *15*, 243–251.
(48) Baumann, L.; Bowditch, R. D.; Baumann, P. *Int. J. Syst. Bacteriol.* **1983**, *33*, 793–802.
(49) Cordiero, A.; Nitschke, M.; Janke, A.; Helbig, R.; D'Souza, F.; Donnelly, G.; Willemsen, P.; Werner, C. *Exp. Polym. Lett.* **2009**, *3*, 70–83.
(50) Gudipati, C. S.; Finlay, J. A.; Callow, J. A.; Callow, M. E.; Wooley, K. L. *Langmuir* **2005**, *21*, 3044–3053.
(51) Zhang, Z.; Finlay, J. A.; Wang, L.; Gao, Y.; Callow, J. A.; Callow, M. E.; Jiang, S. *Langmuir* **2009**, *25*, 13516–13521.
(52) Bers, A. V.; Diaz, E. R.; da Gama, B. A. P.; Vieira-Silva, F.; Dobretsov, S.; Valdivia, N.; Thiel, M.; Scardino, A. J.; McQuaid, C. D.; Sudgen, H. E.; Thomason, J. C.; Wahl, M. *Biofouling* **2010**, *26*, 367–377.
(53) Aldred, N.; Scardino, A.; Cavaco, A.; de Nys, R.; Clare, A. S. *Biofouling* **2010**, *26*, 287–299.
(54) Scardino, A. J.; Zhang, H.; Cookson, D. J.; Lamb, R. N.; de Nys, R. *Biofouling* **2009**, *25*, 757–767.
(55) Scardino, A. J.; Hudleston, D.; Peng, Z.; Paul, N. A.; de Nys, R. *Biofouling* **2009**, *25*, 83–93.
(56) Krishnan, S.; Weinman, C. J.; Ober, C. K. *J. Mater. Chem.* **2008**, *18*, 3405–3413.
(57) Finlay, J. A.; Krishnan, S.; Callow, M. E.; Callow, J. A.; Dong, R.; Asgill, N.; Wong, K.; Kramer, E. J.; Ober, C. K. *Langmuir* **2008**, *24*, 503–510.
(58) Finlay, J. A.; Callow, M. E.; Schultz, M. P.; Swain, G. W.; Callow, J. A. *Biofouling* **2002**, *18*, 251–256.
(59) Finlay, J. A.; Bennett, S. M.; Brewer, L. H.; Sokolova, A.; Clay, G.; Gunari, N.; Meyer, A. E.; Walker, G. C.; Wendt, D. E.; Callow, M. E.; Callow, J. A.; Detty, M. R. *Biofouling* **2010**, *26*, 657–666.
(60) Baier, R. E. *J. Mater. Sci.: Mater. Med.* **2006**, *17*, 1057–1062.